Demonstration by Ultraviolet Resonance Raman Spectroscopy of Differences in DNA Organization and Interactions in Filamentous Viruses Pf1 and fd†

Zai Qing Wen, Andrew Armstrong, and George J. Thomas, Jr.*

Division of Cell Biology and Biophysics, School of Biological Sciences, University of Missouri—Kansas City, Kansas City, Missouri 64110

Received August 17, 1998; Revised Manuscript Received January 8, 1999

ABSTRACT: Pf1, a class II filamentous virus, has been investigated by ultraviolet resonance Raman (UVRR) spectroscopy with excitation wavelengths of 257, 244, 238, and 229 nm. The 257-nm UVRR spectrum is rich in Raman bands of the packaged single-stranded DNA (ssDNA) genome, despite the low DNA mass (6%) of the virion. Conversely, the 229-nm UVRR spectrum is dominated by tyrosines (Tyr 25 and Tyr 40) of the 46-residue α-helical coat subunit. UVRR spectra excited at 244 and 238 nm exhibit Raman bands diagnostic of both viral DNA and coat protein tyrosines. Raman markers of packaged Pf1 DNA contrast sharply with those of the DNA packaged in the class I filamentous virus fd [Wen, Z. Q., Overman, S. A., and Thomas, G. J., Jr. (1997) *Biochemistry 36*, 7810−7820]. Interestingly, deoxynucleotides of Pf1 DNA exhibit sugars in the C2′-*endo/anti* conformation and bases that are largely unstacked, compared with C3′-*endo/anti* conformers and very strong base stacking in fd DNA; hydrogen-bonding interactions of thymine carbonyls are also different in Pf1 and fd. On the other hand, coat protein tyrosines of Pf1 exhibit Raman markers of ring environment identical to those of fd, including an anomalous singlet at 853 cm^{-1} in lieu of the canonical Fermi doublet (850/830 cm^{-1}) found in globular proteins. The results indicate markedly different modes of organization of ssDNA in Pf1 and fd virions, despite similar environments for coat protein tyrosines, and suggest strong hydrogen-bonding interactions between DNA bases and coat subunits of Pf1 but not between those of fd. We propose that structural relationships between the protein coat and encapsidated ssDNA genome are also fundamentally different in the two assemblies.

Pf1 is a long and thin filamentous virus (∼2000 nm length × ∼6 nm diameter) that infects *Pseudomonas aeruginosa* strain K. The mature virion comprises a single-stranded (ss) and covalently closed DNA genome of 7349 nucleotides sheathed by 7350 copies of a 46-residue α-helical subunit (sequence [1]GVIDT SAVQS AITDG QGDMK AIGGY IVGAL VILAV AGLIY SMLRK [46]A) (*1*−*3*). The arrangement of subunits in Pf1 defines a filament architecture (class II) that is distinct from the well-characterized architecture of class I filamentous viruses, such as fd, f1, and M13 (*1*).

The structure of Pf1[1] has been investigated by fiber X-ray diffraction (*4*−*7*), neutron diffraction (*8, 9*), solid-state nuclear magnetic resonance (NMR) spectroscopy (*10, 11*), Raman spectroscopy (*12*−*14*), fluorescence spectroscopy (*15*), and circular dichroism (CD) (*16*) and linear dichroism (LD) methods (*17*). Molecular modeling has also been employed to suggest plausible helical arrangements for the coat protein subunits and their relationship to the packaged ssDNA molecule (*1, 18*). However, details of intersubunit packing, genome organization and putative interactions between the packaged DNA and coat subunits have remained largely unresolved. Because the Pf1 DNA molecule comprises only a small percentage (6%) of the total Pf1 mass, it has represented a particularly formidable challenge to the structural methods applied previously. Up to the present, the Pf1 system has not been investigated by ultraviolet resonance Raman (UVRR) spectroscopy.

Recent application of UVRR spectroscopy to the fd assembly demonstrates that the method combines the sensitivity and selectivity required to probe specific residues of both DNA and coat subunits in a filamentous virus (*19, 20*). In the UVRR approach, the laser-excitation frequency is tuned into resonance with the target chromophore, and thereby the resonance-enhanced Raman spectrum of the chromophore is selectively obtained. Reviews of UVRR applications to biological molecules have been given by Austin et al. (*21*) and Thomas and Tsuboi (*22*). Until recently (*19, 23*−*25*), however, UVRR spectroscopy of nucleoproteins has not been feasible, due principally to limitations in UV laser and detector technologies. Improvements in spectrometer design and performance now permit exploitation of the UVRR method to probe the bases of packaged ssDNA and the aromatic side chains of coat protein subunits in filamentous viruses, despite the fact that these residues represent only a small fraction of the total virion mass.

In this paper, we report the use of UVRR spectroscopy to probe DNA base and coat protein tyrosine environments in the Pf1 assembly. UVRR spectra of Pf1 in H_2O and D_2O solutions were obtained with excitation wavelengths of 257,

† Paper LXVI in the series Structural Studies of Viruses by Laser Raman Spectroscopy. Supported by NIH Grant GM50776.

* To whom correspondence should be addressed.

[1] Abbreviations: CD, circular dichroism; LD, linear dichroism; UV, ultraviolet; UVRR, ultraviolet resonance Raman; NMR, nuclear magnetic resonance; ssDNA, single-stranded DNA; dsDNA, double-stranded DNA.

10.1021/bi981965m CCC: $18.00
Published on Web 02/19/1999

244, 238, and 229 nm. Assignment of UVRR bands has been facilitated by parallel examination of deoxynucleosides and aromatic amino acids using identical laser-excitation wavelengths and sampling protocols (*26*). The results obtained on Pf1 are also discussed in relation to those reported in a recent UVRR investigation of the class I filamentous virus fd (*19*). The present findings indicate that while UVRR markers of tyrosine residues of the Pf1 coat protein are virtually identical to those of the fd coat protein, the UVRR markers of packaged Pf1 and packaged fd DNA molecules are radically different. A quantitative analysis of the UVRR signatures indicates completely different modes of genome organization in the Pf1 and fd filaments.

EXPERIMENTAL PROCEDURES

(1) Materials. Growth medium (LB), standard reagents, amino acids, and nucleosides were obtained from Sigma Chemical Co. (St. Louis, MO) and Fisher Scientific (Pittsburgh, PA). The Pf1 virus was grown on *Pseudomonas aeruginosa* strain K in LB medium using stocks obtained originally from Dr. Loren A. Day, Public Health Research Institute, New York. General procedures for phage isolation, purification, and pelleting for Raman spectroscopic analysis have been described (*13*). The purified virus was pelleted from 10 mM Tris buffer at pH 7.8 and resuspended in the same buffer at 10 mg/mL.

For UVRR measurements, Pf1 solutions were diluted to approximately 4 mg/mL in 10 mM Tris buffer (pH 7.8). D_2O solutions of Pf1 were prepared in an identical manner, except that D_2O replaced H_2O in the pelleting and dilution buffers. Sodium sulfate was added to virus solutions at a nominal concentration of 100 mM for use of the 981 cm^{-1} band of SO_4^{2-} as an internal Raman intensity standard. In each sample preparation the precise Na_2SO_4 concentration was determined gravimetrically. Sodium and sulfate ion concentrations in the range 10−200 mM were found to have no significant effect upon the relative intensities of Raman bands of the viral DNA component.

(2) UVRR Spectroscopy. UVRR spectra were excited at 257, 244, 238, and 229 nm using a continuous-wave, frequency-doubled argon laser (Innova 300 FReD, Coherent Inc., Santa Clara, CA). Laser power at the sample was maintained at approximately 5 mW for excitation at 257 nm and approximately 1 mW for excitations at 244, 238, and 229 nm. Raman scattering at 90° from a custom-designed, rotating (3000 rpm) quartz sample cell was analyzed with a single grating (2400 g/mm) spectrograph (Spex 750M, ISA, Edison, NJ) equipped with a prism predispersive element (McPherson Instruments, Acton, MA) and liquid nitrogen-cooled charge-coupled device detector (ISA, Edison, NJ). The effective spectral resolution was 8 cm^{-1} or less. Further details of the design and performance characteristics of the UVRR instrument have been described (*24*).

Each UVRR spectrum shown in the figures is an average of at least six separately collected spectral accumulations (up to 1 h each, at 20 °C). Raman frequencies were calibrated to ±1 cm^{-1} by using a standard liquid mixture of carbon tetrachloride and acetonitrile. Corrections for the weak UVRR scattering of liquid water, gently sloping background and spurious cosmic rays were carried out as previously described (*24, 26*). Data were processed with Grams software (Galactic Industries, Salem, NH).

UVRR spectra of samples showed no significant time dependence, indicating no appreciable photodecomposition during data collection protocols. Sample integrity was confirmed following UVRR data collections by conventional UV absorption spectroscopy and plaque assays.

(3) Data Analysis: (a) Raman Scattering Cross Sections. The scattering cross section (σ_n) of a Raman band at frequency ν_n may be obtained by comparison of its peak height (I_n) with the peak height (I_s) of an internal standard Raman band at frequency ν_s of known absolute Raman scattering cross section (σ_s):

$$\sigma_n = \sigma_s(I_n/I_s)(C_s/C_n)[(\nu_0 - \nu_s)/(\nu_0 - \nu_n)]^4 \qquad (1)$$

C_s and C_n are the molar concentrations of the internal standard and target molecule (or residue), respectively, and ν_0 is the frequency of the laser exciting line, usually in reciprocal centimeter units. Here, we employ as internal standard the prominent UVRR band of sodium sulfate at 981 cm^{-1}, which is assigned to the symmetrical stretching vibration of the SO_4^{2-} ion. Fodor et al. (*27*) have determined the absolute Raman scattering cross section of the 981 cm^{-1} band of SO_4^{2-} as a function of excitation wavelength in the ultraviolet region. From their results, we find $\sigma_s = 0.42$, 0.32, 0.24, and 0.16 millibarn at 229, 238, 244, and 257 nm, respectively.

In applying eq 1 to a Raman band of a particular nucleoside constituent of DNA, we replace C_n by C_b ($\equiv X_b C_n$, where X_b is the base mole fraction in DNA). C_b is estimated from the UV absorbance of the DNA at 260 nm. For the packaged Pf1 genome, the molar concentration of a particular base is obtained from

$$C_b = X_b C_n = X_b W f / M_{nuc} \qquad (2)$$

where W is the weight concentration of the virion, which can be determined from the UV absorption spectrum and published extinction coefficients, f is the nominal weight fraction of DNA in the virion, and M_{nuc} is the average nucleotide molecular weight.

In evaluating the Raman scattering cross section of a tyrosine band of Pf1, we obtain the molar concentration of tyrosine (C_{Tyr}) by making use of the known nucleotide/subunit ratio (1.0) and the number of tyrosines per subunit (*2*). Thus, C_{Tyr}:C_n = 2:1.

(b) Raman Hypochromic Effects. It is well-known that Raman scattering cross sections for certain ring vibrational modes of purine and pyrimidine bases in double-helical nucleic acids can be significantly smaller than those of corresponding nucleosides, a phenomenon referred to as Raman *hypochromism* (*28, 29*). Raman hypochromic effects have been attributed to stacking interactions of the nucleic acid bases that depress electronic extinction coefficients and hence diminish the corresponding Raman intensities upon which they are dependent (*29*).

We define the fractional hypochromicity of a DNA Raman band at frequency n by the relation $1 - \gamma_n^{DNA}$, where the hypochromic ratio, γ_n^{DNA}, is the quotient of intensities in Raman spectra of the nucleic acid and constituent nucleosides. The term hypochromism properly refers to cases where $\gamma_n^{DNA} < 1$; conversely, *hyperchromism* implies $\gamma_n^{DNA} > 1$. In terms of the corresponding Raman scattering cross

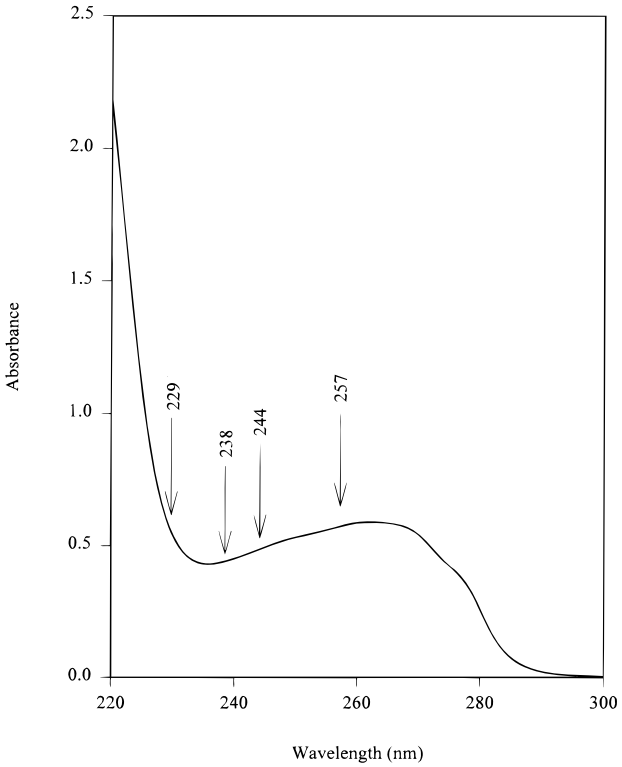

FIGURE 1: Ultraviolet absorption spectrum of Pf1 virus in the wavelength interval 220−300 nm. Arrows indicate the laser wavelengths used to excite ultraviolet resonance Raman (UVRR) spectra displayed in subsequent figures. Virus concentration is approximately 1.5 mg/mL and the optical path is 2 mm.

sections, γ_n^{DNA} is given by

$$\gamma_n^{DNA} \equiv I_n^{DNA}/I_n^{nuc} = \sigma_n^{DNA}/\sigma_n^{nuc} \quad (3)$$

where σ_n^{DNA} and σ_n^{nuc} are Raman scattering cross sections for the band in DNA and in a solution of the free nucleoside, respectively.

By analogy with eq 3, we may similarly define γ_n^{prot} for a Raman band of a protein aromatic residue:

$$\gamma_n^{prot} \equiv I_n^{prot}/I_n^{aa} = \sigma_n^{prot}/\sigma_n^{aa} \quad (4)$$

where σ_n^{prot} and σ_n^{aa} are Raman scattering cross sections for the residue in the protein and in a solution of the free amino acid.

(c) Experimental Uncertainties. The Raman scattering cross sections reported below are averages of multiple independent experiments exhibiting deviations of ±10% or less. These deviations reflect uncertainties in band intensity measurements, which are due mainly to spectral noise and baseline determinations. Other potential sources of error, such as spectrograph polarization effects and sample photodecomposition, are virtually eliminated by the experimental design and data collection protocols, as previously described (*24, 26*).

RESULTS AND DISCUSSION

(1) Assignment of Raman Bands in UVRR Spectra of Pf1. Figure 1 shows the UV absorption profile of Pf1 in the spectral interval 220−300 nm and the four laser wavelengths employed for excitation of UVRR spectra of the virus. The UVRR spectra (600−1800 cm^{-1}) of Pf1 in H_2O and D_2O solutions are shown in Figures 2 and 3, respectively. The data of Figures 2 and 3 illustrate the strong dependence of the Pf1 UVRR spectrum upon excitation wavelength. Thus, the UVRR spectrum excited at 229 nm is due virtually exclusively to coat protein tyrosines, Tyr 25 and Tyr 40. Conversely, the UVRR spectrum excited at 257 nm is due predominantly to bases of packaged Pf1 DNA and exhibits only very small contributions from coat protein tyrosines. The UVRR spectra excited at 238 and 244 nm contain significant contributions from both the tyrosines and DNA bases. These results are in accord with the known contributions of coat protein tyrosines and packaged DNA to the UV absorption spectrum of the native virus (*16*).

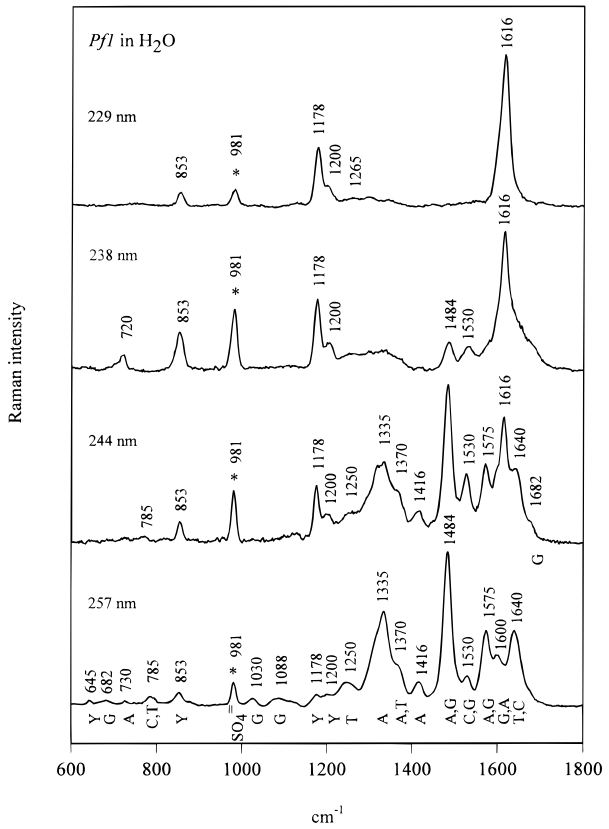

FIGURE 2: From top to bottom: UVRR spectra of H_2O solutions of Pf1 virus, excited at 229, 238, 244, and 257 nm. Sample concentrations in terms of moles of DNA nucleotides packaged are 0.40, 0.44, 0.42, and 0.52 mM, respectively (1 mM base concentration corresponds to 5.4 mg of virus/mL). The internal standard used for intensity calculations is the 981 cm^{-1} band of Na_2SO_4. The respective Na_2SO_4 concentrations are 250, 111, 62, and 42 mM. UVRR spectra were obtained with laser powers of ~1 mW at 229, 238, and 244 nm and ~5 mW at 257 nm.

Interestingly, despite the very low mass of DNA (6 wt %) in the Pf1 virion, Raman markers of the nucleotide bases are intense and numerous in spectra excited at 257 and 244 nm. On the other hand, the sugar−phosphate backbone of Pf1 DNA, as well as the nonaromatic side chains and polypeptide backbone of Pf1 coat protein, do not contribute to any of the spectra of Figures 2 and 3. This is due to the fact that UV extinction coefficients for these moieties, and therefore their resonance Raman scattering cross sections, are too low in comparison to those of the DNA bases and coat protein tyrosines to be detected at the experimental conditions employed.

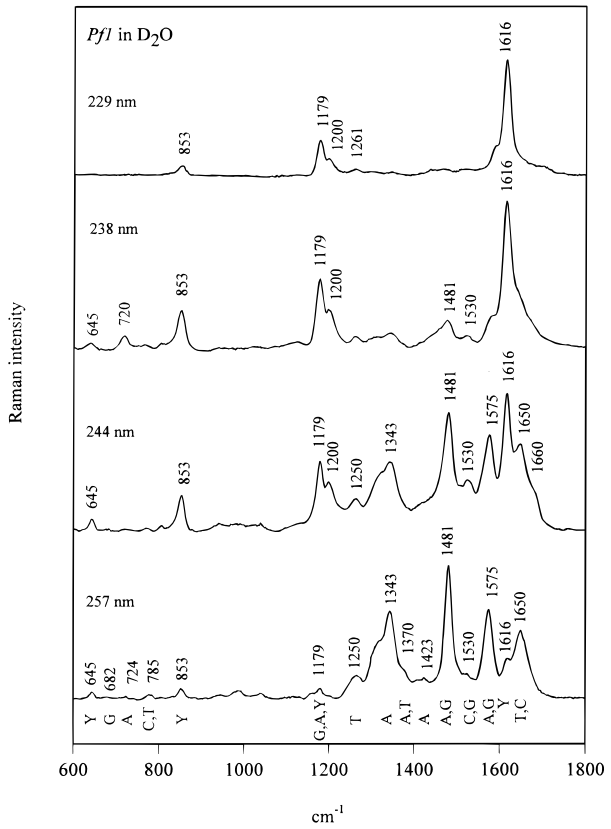

FIGURE 3: From top to bottom: UVRR spectra of D_2O solutions of Pf1 virus, excited at 229, 238, 244, and 257 nm. Sample concentrations in terms of moles of DNA nucleotides packaged are 0.38, 0.48, 0.45, and 0.50 mM, respectively. Other conditions are as given in Figure 2.

Table 1 summarizes Raman band assignments of Pf1 in UVRR spectra excited at 257, 244, 238, and 229 nm. The assignments of Table 1 are consistent with previously reported off-resonance Raman spectra of Pf1 (*12, 13)* and UVRR spectra obtained from constituent deoxynucleosides and amino acids (*21, 26, 27, 30*−*37*). Deuteration shifts observed in the 257-nm-excited UVRR spectrum of Pf1 (indicated in parentheses in the first column of Table 1) are also in accord with the proposed assignments. A complete tabulation of 257-, 244-, 238-, and 229-nm-excited UVRR frequencies and Raman band cross sections for H_2O solutions of the nucleosides and amino acids has been given elsewhere (*26*). (A comprehensive tabulation, including data from corresponding D_2O solutions, is available upon request from the authors.)

(2) Structurally Informative Raman Bands of the Packaged Pf1 Genome. (a) The 1640 cm^{-1} *Band: Pyrimidine Carbonyl Hydrogen Bonding.* A striking feature of the 257-nm spectrum of Pf1 is the Raman band at 1640 cm^{-1} (Figure 2, bottom trace). This band must originate from base residues of packaged Pf1 DNA, because no other viral constituent is expected to contribute a resonance-enhanced Raman marker of comparable frequency or intensity (*19, 26, 37*). Furthermore, of the four DNA bases, adenine has no UVRR band above 1603 cm^{-1}, and guanine has none between 1603 and 1660 cm^{-1} (*26*). Accordingly, the only plausible assignment is to thymine and/or cytosine residues, which normally exhibit C═O stretching bands in the 1650−1655 cm^{-1} interval of the 257-nm spectrum (*26*). Thymine is clearly the much greater contributor to this region of the UVRR

Table 1: Raman Assignments of Pf1 Virus in UVRR Spectra Excited at 257, 244, 238, and 229 nm[a]

257 nm	244 nm	238 nm	229 nm	residue[b]	type of mode[c]
645	645	645		Tyr	*Y6b*
682				G	ring s
		720		Tyr	*Y13*
730 (−4)				A	ring s
785				C, T	ring s
853	853	853	853	Tyr	ring s
1030				G	
1088				G	
1178 (+1)	1178	1178	1178	Tyr	*Y9a*
1200	1200	1200	1200	Tyr	*Y7a*
1250	1250			T	C2N3 s
			1265 (−4)	Tyr	*Y7a′*
1335 (+8)	1335	1335		A	N7C5, C8N7 s
1370	1370			A, T	C1N9 s, C6N6 s
1416 (+7)	1416			A	C4C9 s, C8H d
1484 (−2)	1484	1484		A, G	C2H d, N9C8 s
1530	1530	1530		C, G	N3C4 s
1575	1575			G, A	C5C4, C4C3 s
1600 (−421)				G, A	C5C6 s, NH_2 d
	1616	1616	1616	Tyr	*Y8a*
1640 (+10)	1640			T, C	C4═O, C5═C6 s
	1682 (−22)			G	C6═O, N1H d

[a] For the excitation wavelengths indicated at the top of columns 1−4, the UVRR frequencies of H_2O solutions are listed in reciprocal centimeter units. Values in parentheses indicate deuteration shifts observed for corresponding D_2O solution spectra. [b] A, C, G, and T indicate DNA bases; Tyr indicates tyrosine. [c] Vibrational assignments and nomenclature are from model compound studies (*21, 26*−*37*). Abbreviations: s, stretching; d, deformation.

spectrum. Its C═O marker band, which originates mainly from the C4═O group stretching vibration, has a 5-fold larger UVRR cross section (normalized intensity) than the cytosine C2═O marker band (*26*) and is therefore the logical assignment. The 1640 cm^{-1} band of Pf1, however, is surprisingly low in frequency compared with the thymidine band observed in the free deoxynucleoside (1655 cm^{-1}) or in an aqueous deoxynucleoside mixture with the same base composition as Pf1 DNA (1653 cm^{-1}) (Figure 4, left panel). The Pf1 band is also much lower in frequency than the corresponding band (1650 cm^{-1}) of unpackaged ssDNA or dsDNA (*19*). Because this displaced Pf1 band is assignable predominantly to thymine C4═O groups (with only a small contribution possible from cytosine C2═O groups), we conclude that pyrimidine carbonyl acceptors of packaged Pf1 DNA exist in a substantially different local environment than occurs for either aqueous deoxynucleosides or protein-free DNA. On the basis of studies of many model hydrogen-bonding systems (*38*), the displacement of the C4═O band to lower frequency by 10−13 cm^{-1} compared with other DNA can be considered diagnostic of the formation of much stronger hydrogen bonds.

A similar displacement to lower frequency is observed for the C═O band of packaged Pf1 DNA in D_2O. Thus, the thymine C═O marker of deuterated Pf1 appears at 1650 cm^{-1}, compared with 1658 cm^{-1} in the D_2O solution mixture of deoxynucleosides having the Pf1 DNA base composition (Figure 4, right panel). Interestingly, all other Raman bands of packaged Pf1 DNA exhibit frequencies that are within experimental uncertainty (±2 cm^{-1}) of those in the deoxynucleoside mixture (Figure 4).

(b) The 1682 cm^{-1} *Band: Guanine C6═O and N1H Environments.* Another useful structural marker of Pf1 DNA occurs at 1682 cm^{-1} in the 244-nm spectrum (Figure 2).

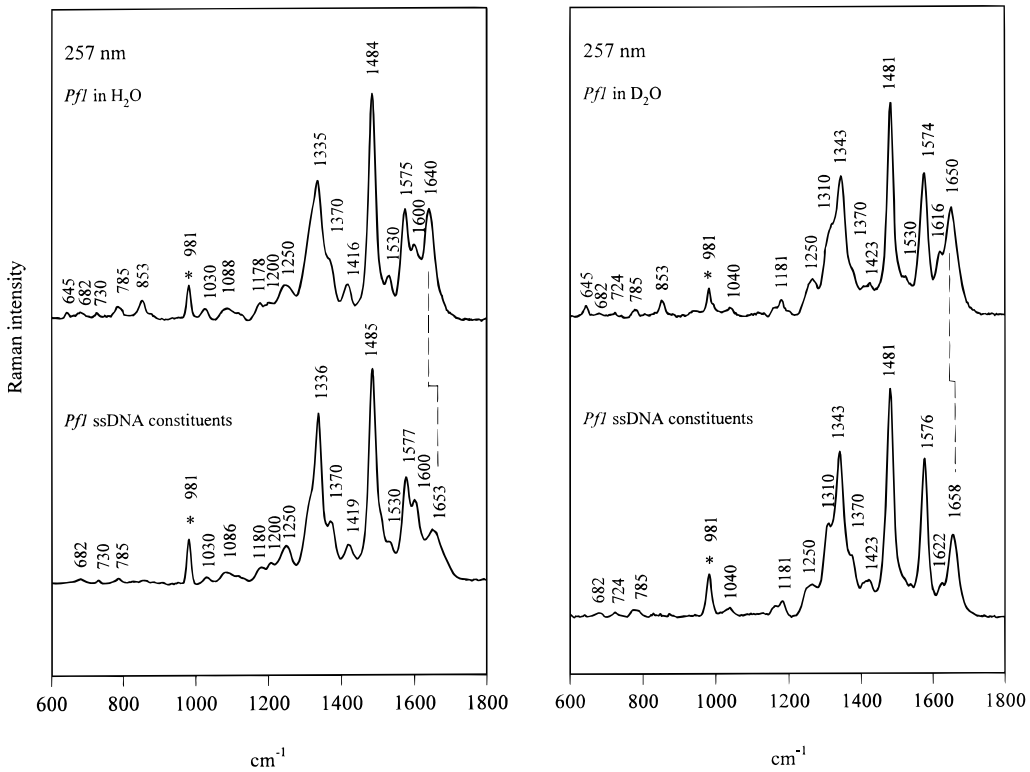

FIGURE 4: Left panel: UVRR spectra (257 nm) of H_2O solutions of Pf1 (top) and a deoxynucleoside mixture (19% dA, 20% dT, 33% dG, and 28% dC) corresponding to the base composition of Pf1 DNA (bottom). Sample concentrations in terms of moles of DNA nucleotides are 0.52 and 0.30 mM, respectively, and Na_2SO_4 concentrations are 42 and 50 mM, respectively. Right panel: UVRR spectra (257 nm) of D_2O solutions of Pf1 (top) and the deoxynucleoside mixture corresponding to the base composition of Pf1 DNA (bottom). Sample concentrations in terms of moles of DNA nucleotides are 0.65 and 0.80 mM, respectively, and Na_2SO_4 concentrations are 50 and 100 mM, respectively.

Deoxyguanosine residues are the only significant contributors to this band (*26*). We find that the 1682 cm^{-1} marker is deuteration-shifted to 1660 cm^{-1} (Figure 3), consistent with its assignment to a vibrational mode involving mainly guanine C6═O stretching and an additional contribution from N1H in-plane bending (*26, 39*). The Raman frequency of this guanine marker is known to be highly sensitive to base associations (*40*). For example, in DNA structures containing Watson−Crick pairs or Hoogsteen quartets, the band is observed well above 1700 cm^{-1} (*39*). Conversely, when guanine is not paired with cytosine and not involved in quartet formation but is associated with other hydrogen-bonding agents (including water molecules), the band is observed as low as 1682 cm^{-1} (*39, 40*). Evidently, guanines of the packaged Pf1 genome do not participate in interbase associations but in other C6═O and N1H hydrogen-bonding interactions.

(c) The 682 cm^{-1} Band: Deoxyguanosine Conformation. An important although weak DNA marker is observed at 682 cm^{-1} in 257-nm UVRR spectra of Pf1 in both H_2O and D_2O solutions (Figures 2 and 3). Amplification of this region of the spectrum is shown in Figure 5. Insensitivity of the 682 cm^{-1} band to deuteration confirms its assignment to deoxyguanosine residues of packaged DNA and identifies the dG conformation as C2′-*endo/anti* (*22, 26, 41*). This finding is consistent with the conclusion reached independently from off-resonance Raman spectra of Pf1 (*13*). Implications of C2′-*endo/anti* dG in Pf1 DNA are discussed below.

(d) Raman Hypochromic Effects and Base Stacking Interactions. Ring vibrations of the DNA purines generate strong Raman bands at 1335 (A), 1484 (A, G) and 1575 (G, A) cm^{-1}. The UVRR cross sections of these bands are sensitive to base stacking interactions (*19, 42*). Table 2 lists the UVRR cross sections for the 1335, 1484, and 1575 cm^{-1} bands in the 257-nm excited spectrum of packaged Pf1 DNA, calculated from data of Figure 2 in accordance with eqs 1 and 2. By use of eq 3, these Pf1 data are compared with corresponding cross sections for the aqueous deoxynucleoside mixture (Figure 4) to yield the hypochromic ratios (γ) given in Table 2. We find that for the packaged Pf1 DNA molecule, the 1335 cm^{-1} band intensity is diminished by 42% (γ = 0.58), while intensities of the 1484 and 1575 cm^{-1} bands are diminished, respectively, by only 14% and 18%. All of these hypochromic effects are small in comparison to those of packaged fd DNA, where the counterpart UVRR bands suffer intensity losses of 75% or greater (Table 2). It is interesting to note that the hypochromic effects observed here for packaged Pf1 DNA are also small in comparison to those (∼60%) of double-stranded (ds) DNA examined at the same experimental conditions (*19*). The present results indicate that purine base stacking in packaged Pf1 DNA is far less extensive than occurs in either packaged fd DNA or in Watson−Crick-paired dsDNA, consistent with previously reported CD results (*16*).

(3) Structurally Informative Raman Bands of the Coat Protein Tyrosines. The spectrum of Pf1 excited at 229 nm (Figure 2, top) contains Raman markers exclusively from the coat protein tyrosines, Tyr 25 and Tyr 40 (*19, 26*). [DNA bands with significant UVRR cross sections at 229 nm are those of cytosine at 1530 cm^{-1} and guanine at 1484 cm^{-1} (*26*), and these are far too weak in comparison to Raman

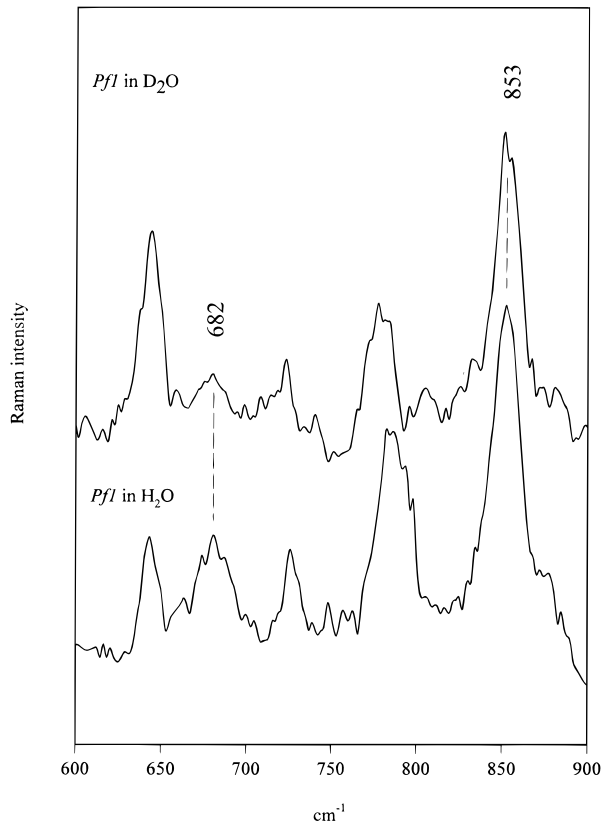

FIGURE 5: UVRR spectra (257 nm) in the 600−900 cm^{-1} interval of Pf1, demonstrating the well-characterized Raman marker of the C2′-*endo/anti* dG conformation at 682 cm^{-1} (*41*) and the tyrosine singlet at 853 cm^{-1} (*44*) in both H_2O (bottom) and D_2O (top) solutions.

Table 2: DNA Raman Hypochromic Ratios (γ) Determined from UVRR Cross Sections in Pf1 and fd Viruses (σ^{DNA}) and Deoxynucleoside Mixtures (σ^{nuc})[a]

	Pf1 virus			fd virus		
band (cm^{-1})	σ^{DNA}	σ^{nuc}	γ	σ^{DNA}	σ^{nuc}	γ
1335	222	381	0.58	83	395	0.21
1484	198	230	0.86	60	244	0.25
1575	80	97	0.82	17	70	0.24
1640/1646/1652[b]	200	120	1.70	32	110	0.29

[a] Cross sections for bands assigned to packaged DNA (σ^{DNA}) and nucleoside bases (σ^{nuc}) are in millibarn units; hypochromic ratios are defined by eq 3. All data pertain to UVRR spectra excited at 257 nm. [b] This thymine marker is observed at 1640, 1646, or 1652 cm^{-1}, respectively, in packaged Pf1 DNA, packaged fd DNA, or the free nucleoside.

bands of tyrosine to appear in the 229-nm spectrum of Figure 2.] UVRR markers of Pf1 tyrosines differ dramatically from those of the free amino acid (*26*). Thus, the components of the phenolic ring Fermi doublet (2*Y16a*+*Y1*), which occur near 850 and 830 cm^{-1} for free tyrosine and for tyrosine side chains in all globular proteins heretofore examined (*43*), are supplanted in Pf1 by a singlet at 853 cm^{-1} (Figure 5). Therefore, both Tyr 25 and Tyr 40 generate a tyrosine singlet at 853 cm^{-1}. A similar anomaly has been reported previously for the two tyrosines (Tyr 21 and Tyr 24) of the native fd virion subunit (*19, 44*). As in the case of fd, the 853 cm^{-1} singlet exhibited by each tyrosine of the Pf1 virion subunit is attributed to an unusual hydrophobic environment for the phenolic ring within the native virion assembly.

Table 3: Tyrosine Hyperchromic Ratios (γ) Determined from UVRR Cross Sections of Pf1 Coat Protein Tyrosines ($\sigma^{Tyr25/Tyr40}$) and L-Tyrosine ($\sigma^{L-tyrosine}$)[a]

band (cm^{-1})	$\sigma^{Tyr25/Tyr40}$	$\sigma^{L-tyrosine}$	γ
853	104	61	1.7
1178	457	254	1.8
1200	180	106	1.7
1616	1115	587	1.9

[a] Cross sections are in millibarn units. Hyperchromic ratios are defined by eq 4. All data pertain to UVRR spectra excited at 229 nm.

Raman cross sections for marker bands of the Pf1 tyrosines (including the cross section for the 853 cm^{-1} singlet) are nearly 2-fold greater than those of aqueous L-Tyr (*26*). The tyrosine Raman markers of Pf1 thus exhibit Raman *hyper*-chromism with respect to the free amino acid. The relevant data are compiled in Table 3. The enhanced Tyr 25 and Tyr 40 UVRR intensities are as expected for highly hydrophobic aromatic ring environments (*45*, *46*) and are consistent with the phenolic environments proposed for the Pf1 assembly.

Comparison of UVRR spectra of Pf1 in H_2O and D_2O solutions (Figures 2 and 3) shows that the tyrosine marker appearing at 1265 cm^{-1} in H_2O is shifted to 1261 cm^{-1} in D_2O. The 1265 cm^{-1} band is assigned to tyrosine normal mode *Y7a*′, which involves phenolic C−O stretching (*34*). A smaller deuteration shift is expected and observed (+1 cm^{-1}) for the tyrosine marker at 1178 cm^{-1}, assigned to normal mode *Y9a* and involving COH bending (*26*, *34*, *47*). The deuteration shifts of *Y7a*′ and *Y9a* confirm that phenolic OH groups of Tyr 25 and Tyr 40 are exchanged by D_2O solvent, notwithstanding the hydrophobic ring environments. The Pf1 tyrosine Raman markers and their deuteration shifts are similar to those of fd (*19*, *44*, *47*), implying similar environments in both assemblies.

Despite the many spectral similarities between tyrosines of Pf1 and fd, a significant difference does occur in the Raman marker corresponding to normal mode *Y7a*, which is observed at 1200 ± 1 cm^{-1} in Pf1 (Figure 2) and 1205 ± 1 cm^{-1} in fd (*19*, *44*, *47*). In model tyrosines, *Y7a* occurs at 1209 cm^{-1} and is deuteration insensitive (*19*, *26*, *35*, *47*). Because the normal mode in question involves stretching of the phenolic ring linkage to Cβ (*26*, *34*, *35*), the observed frequency differences among Pf1, fd, and model tyrosines may be attributed to different ring orientations in the respective structures. The orientations of Tyr 21 and Tyr 24 side chains in fd have been determined experimentally (*48*), but those of Tyr 25 and Tyr 40 in Pf1 remain under investigation by polarized Raman methods (unpublished results of S. A. Overman, M. Tsuboi, Z. Q. Wen, and G. J. Thomas, Jr.). Differences in tyrosine side-chain orientations in the two filament assemblies would be consistent with results of model-building studies based upon fiber X-ray diffraction data (*1*, *4*, *6*, *18*, *49*).

(4) UVRR Signatures of Deuterium Exchange of the Pf1 Virion. It is of interest to examine the exchangeability of amino and imino protons of the DNA bases of Pf1 when the virus is dissolved in D_2O. Figure 3 shows UVRR spectra of D_2O solutions of Pf1 excited at 257, 244, 238, and 229 nm, for comparison with the corresponding H_2O solution spectra of Pf1 shown in Figure 2. The observed deuteration shifts, 1600 → 1179 cm^{-1} (dG, dA), 1640 → 1650 cm^{-1} (dT), 1484 → 1481 cm^{-1} (dG), and 1335 → 1343 cm^{-1} (dA),

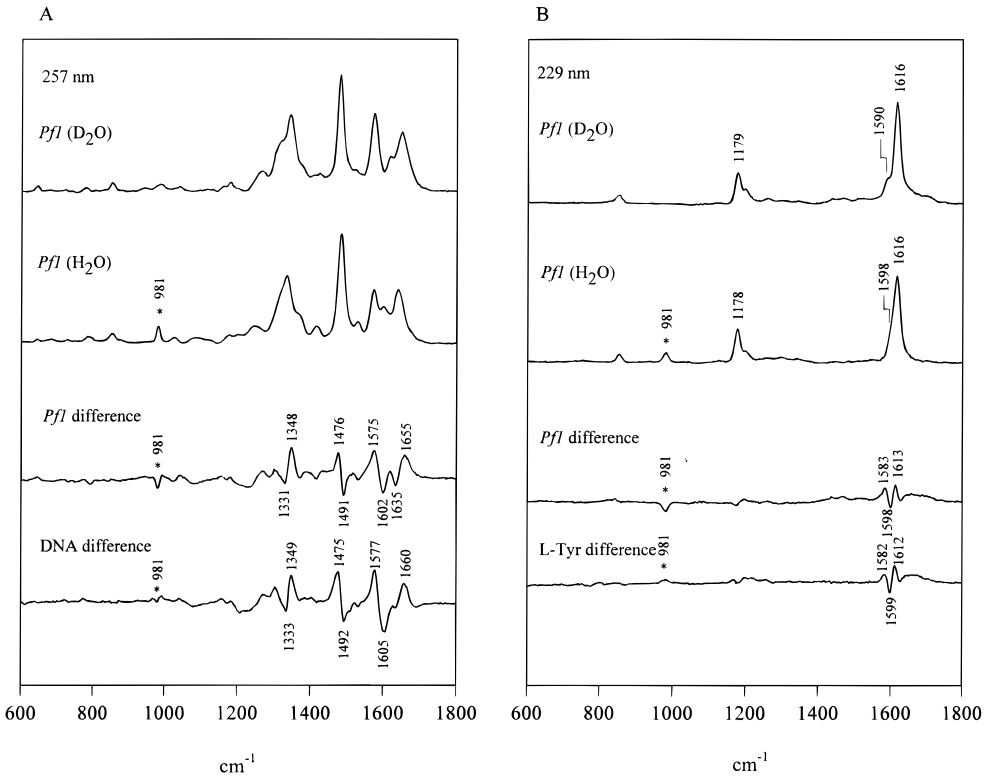

FIGURE 6: Left panel (A): UVRR spectra (257 nm) of Pf1 in D_2O (top) and H_2O (second from top) and their difference spectrum (second from bottom). Also shown for comparison (bottom) is the D_2O-minus-H_2O difference spectrum of Pf1 DNA nucleotides. Right panel (B): UVRR spectra (229 nm) of Pf1 in D_2O (top) and H_2O (second from top) and their difference spectrum (second from bottom). Also shown for comparison (bottom) is the D_2O-minus-H_2O difference spectrum of L-tyrosine. Data are at pH/pD 7.5 ± 0.3.

confirm that base amino and imino sites are fully exchanged in the time interval of the experiments (~2 h). These results are similar to those reported previously for deuterium exchange of packaged fd DNA (*19*, *47*) and indicate that solvent molecules readily penetrate the protein coats of both the Pf1 and fd filaments.

Figure 6 compares UVRR difference spectra of D_2O and H_2O solutions of Pf1, at the two most informative excitation wavelengths, 257 (panel A) and 229 nm (panel B). In both cases, the observed virus difference spectrum is virtually identical to that of the isolated viral constituent generating the bands, clearly demonstrating complete deuteration of bases of packaged ssDNA (Figure 6A) and tyrosines of the coat protein (Figure 6B). The data also illustrate the advantage of UVRR over off-resonance Raman spectroscopy (*47*) in resolving specific H → D exchanges of the genome and subunit tyrosines from more complex amide exchange phenomena of the coat assembly. Like fd (*47*), Pf1 exhibits a complicated time-dependent amide H → D exchange profile, to be reported in detail elsewhere (A. Armstrong, S. A. Overman, Z. Q. Wen, and G. J. Thomas, Jr., manuscript in preparation).

CONCLUSIONS AND SUMMARY

UVRR spectra of the class II filamentous virus Pf1 have been obtained at four excitation wavelengths: 257, 244, 238, and 229 nm. The UVRR spectrum excited at 257 nm, which is dominated by Raman markers of the packaged ssDNA genome, is unique among reported UVRR fingerprints of DNA, including that of the packaged ssDNA genome of the class I filamentous virus fd. The data, which are consistent with earlier off-resonance Raman studies of filamentous viruses (*12*−*14*), are interpreted as evidence of fundamental differences in the organization of ssDNA molecules in Pf1 and fd filaments.

Remarkable features of the UVRR spectra of Pf1 are the absence of significant hypochromism for bands of packaged ssDNA and substantial hyperchromism for bands of the coat protein tyrosines. The observations imply minimal base stacking and tyrosine intercalation in Pf1. This conclusion is consistent with the large base rise (6 Å) proposed in model-building studies (*1*, *2*) and with results obtained in UV absorption and CD studies (*16*).

UVRR and off-resonance Raman spectra of Pf1 and fd demonstrate many structural similarities for their respective coat protein tyrosines. Both types of spectra indicate strongly hydrophobic ring environments, solvent-exchangeable OH groups, and an anomalous Raman singlet at 853 cm^{-1} (Figure 5). However, a subtle difference is observed in a putative Raman marker (1200−1210 cm^{-1} interval) of tyrosine side-chain orientation.

The UVRR band of Pf1 at 1640 cm^{-1}, which is assigned to thymines of the packaged ssDNA genome (*26*, *37*), is unusually low in frequency compared with corresponding thymine markers in the free deoxynucleoside (1655 cm^{-1}), free ssDNA (1650 cm^{-1}), calf thymus dsDNA (1650 cm^{-1}), or fd virus (1646 cm^{-1}). This indicates that the average local environment for thymine C4═O groups in packaged Pf1 DNA differs considerably from those of thymines in packaged fd DNA and of thymines hydrogen-bonded to either adenine or to H_2O molecules. The precise nature of the unusual DNA thymine environment in Pf1 is not known. However, correlations of vibrational spectral frequencies with hydrogen-bonding strength (*38*) suggest that thymine C4═O

Table 4: Raman and UVRR Determined Structural Properties of Packaged fd DNA and Pf1 DNA[a]

structural feature	packaged fd DNA	packaged Pf1 DNA	reference
base stacking	extensive	minimal	this work
base pairing	none	none	this work, *19*
dG conformation	C3′-*endo/anti*[b]	C2′-*endo/anti*[b]	this work, *14*, *19*
H-bonding of dT	moderate	very strong	this work, *19*
H-bonding of dG	(not detected)	moderate	this work, *19*

[a] Additional dissimilarities between packaged ssDNA genomes of Pf1 and fd, proposed on the basis of other biochemical and biophysical methods, are reviewed elsewhere (*2*, *15*−*17*, *50*). [b] Other deoxynucleosides (dT, dA, and dC) probably assume the same conformation as dG.

groups in Pf1 are acceptors of unusually strong hydrogen bonds. This could result from interactions between thymine C4═O acceptors and coat protein donor groups (such as Arg 44 and Lys 45), which may be located at the DNA−protein interface. It is interesting to note that the packaged Pf1 DNA molecule also exhibits a guanine marker at 1682 cm^{-1}, distinguishing guanine environments of Pf1 DNA from those of other DNA assemblies including duplex and quadruplex structures. The 1682 cm^{-1} marker is consistent with C6═O and N1H hydrogen-bonding interactions with coat subunits.

It is well established from fiber X-ray diffraction studies (*4*−*7*) that symmetrically different subunit arrangements occur in fd (class I) and Pf1 (class II) virions, despite the rather similar helical secondary structures of their respective coat subunits (*12*, *13*). The present UVRR study of Pf1, as well as previous spectroscopic studies of both fd and Pf1 (*10*−*16*, *50*, *51*), provide a consistent body of evidence that *DNA structures in native Pf1 and fd filaments are distinctively different*. Salient differences between packaged fd DNA and packaged Pf1 DNA structures revealed by the Raman and UVRR spectra are summarized in Table 4.

The different DNA structures in Pf1 and fd imply different modes of organization of the viral genomes with respect to the coat protein, and therefore differences in protein−DNA interactions. Although it is not clear at present why qualitatively different coat protein−ssDNA interaction mechanisms should prevail in Pf1 and fd, the UVRR data do not conflict with previously proposed models that attribute such a distinction to the organization of the ssDNA loop itself (*1*). On the other hand, models based upon nonspecific (electrostatic) interactions as the sole basis for assembly of both viruses (*18*) cannot account for the strikingly different UVRR profiles of packaged Pf1 DNA and fd DNA.

With respect to the stability of packaged ssDNA in the filamentous viruses, it is interesting to note that the type of deoxynucleoside sugar pucker and glycosyl orientation found in Pf1 is C2′-*endo/anti*. This type of deoxynucleoside conformation is associated with the lowest energy state of DNA, i.e., B-DNA. Conversely, the deoxynucleoside conformation found in fd is C3′-*endo/anti*, which occurs in the less stable A form of DNA. Thus, Pf1 and fd are distinguished not only by different coat protein symmetries and different protein−DNA interfaces but also by different deoxynucleoside conformations of the ssDNA packaged within. Evidently, the ssDNA deoxynucleoside conformation stabilized within the protein coat of the filamentous virion is not self-conferred but is related to the organization of the protein coat. It seems reasonable to conclude that the DNA residues and coat protein subunits interact specifically and directly with one another. Interactions with other factors, such as counterions and solvent, may also occur.

The present results indicate that the organization of ssDNA in filamentous viruses is fundamentally different than that of dsDNA in icosahedral viruses, such as T7 (*52*, *53*) and P22 (*54*). In both T7 and P22, the packaged dsDNA genome exhibits the same B-form secondary structure that is found in the unpackaged state, and no perturbation of deoxynucleosides from the C2′-*endo/anti* conformation can be detected. In addition, the dsDNA genome in either T7 or P22 does not interact to a significant extent with capsid subunits, although stabilizing interactions with packaged counterions (Mg^{2+}) are clearly evident (*52*, *54*). In the icosahedral dsDNA phages, extensive subunit−DNA interactions are apparently not required to protect the genome from environmental insults. Conversely, in the filamentous virus fd, the packaged ssDNA genome is characterized by the C3′-*endo/anti* deoxynucleoside conformation, a significant perturbation from the C2′-*endo/anti* conformation found in unpackaged fd DNA (*19*). Moreover, an entirely different situation prevails in Pf1, where hydrogen-bonding groups of the bases are dramatically altered with respect to those of unpackaged DNA (Table 4). We conclude that coat subunits of the filamentous viruses protect the encapsidated ssDNA molecule in an assembly-specific manner through subunit−DNA interaction.

ACKNOWLEDGMENT

We thank our colleagues Drs. James M. Benevides and Stacy A. Overman for helpful discussions.

REFERENCES

1. Liu, D. J., and Day, L. A. (1994) *Science 256*, 671−674.
2. Day, L. A., Marzec, C. J., Reisberg, S. A., and Casadevall, A. (1988) *Annu. Rev. Biophys. Biophys. Chem. 17*, 509−539.
3. Hill, D. F., Short, N. J., Perham, R. N., and Peterson, G. B. (1991) *J. Mol. Biol. 218*, 351−364.
4. Marvin, D. A., Nave, C., Bansal, M., Hale, R. D., and Salje, E. K. H. (1992) *Phase Transitions 39*, 45−80.
5. Marvin, D. A., Hale, R. D., Nave, C., and Citterich, M. H. (1994) *J. Mol. Biol. 235*, 260−286.
6. Gonzalez, A., Nave, C., and Marvin, D. A. (1995) *Acta Crystallogr. D51*, 792−804.
7. Makowski, L. (1984) in *Biological Macromolecules and Assemblies* (McPherson, A., Ed.) Vol. 1, pp 203−253, Wiley, New York.
8. Nambudripad, R., Stark, W., Opella, S. J., and Makowski, L. (1991) *Science 252*, 1305−1308.
9. Nambudripad, R., Stark, W., and Makowski, L. (1991) *J. Mol. Biol. 220*, 359−379.
10. Cross, T. A., Tsang, P., and Opella, S. J. (1983) *Biochemistry 22*, 721−725.
11. Shon, K. J., Kim, Y., Colnago, L. A., and Opella, S. J. (1991) *Science 252*, 1303−1305.
12. Thomas, G. J., Jr., and Murphy, P. (1975) *Science 188*, 1205−1207.
13. Thomas, G. J., Jr., Prescott, B., and Day, L. A. (1983) *J. Mol. Biol. 165*, 321−356.

14. Thomas, G. J., Jr., Prescott, B., Opella, S. J., and Day, L. A. (1988) *Biochemistry 27*, 4350−4357.
15. Day, L. A., Wiseman, R. L, and Marzec, C. J. (1979) *Nucleic Acids Res. 7*, 1393−1403.
16. Kostrikis, L. G., Liu, D. J., and Day, L. A. (1994) *Biochemistry 33*, 1694−1703.
17. Clack, B. A., and Gray, D. M. (1992) *Biopolymers 32*, 795−810.
18. Marvin, D. A. (1990) *Int. J. Biol. Macromol. 12*, 125−138.
19. Wen, Z. Q., Overman, S. A., and Thomas, G. J., Jr. (1997) *Biochemistry 36*, 7810−7820.
20. Takeuchi, H., Matsuno, M., Overman, S. A., and Thomas, G. J., Jr. (1996*) J. Am. Chem. Soc. 118*, 3498−3507.
21. Austin, J. C., Jordan, T., and Spiro, T. G. (1993) in *Advances in Spectroscopy* (Clark, R. J. H., and Hester, R. E., Eds.) Vol. 20A, pp 55−127, John Wiley and Sons, New York.
22. Thomas, G. J., Jr., and Tsuboi, M. (1993) *Adv. Biophys. Chem. 3*, 1−70.
23. Asher, S. A., Bormett, R. W., Chen, X. G., Lemmon, D. H., Cho, N., Peterson, P., Arrigoni, M., Spinelli, L., and Cannon, J. (1993) *Appl. Spectrosc. 47*, 628−633.
24. Russell, M. P., Vohník, S., and Thomas, G. J., Jr. (1995) *Biophys. J. 68*, 1607−1612.
25. Tuma, R., Bamford, J. H. K., Bamford, D. H., Russell, M. P., and Thomas, G. J., Jr. (1996) *J. Mol. Biol. 257*, 87−101.
26. Wen, Z. Q., and Thomas, G. J., Jr. (1997) *Biopolymers 45*, 247−256.
27. Fodor, S. P. A., Copeland, R. A., Grygon, C. A., and Spiro, T. G. (1989) *J. Am. Chem. Soc. 111*, 5509−5518.
28. Peticolas, W. L., Kubasek, K. L., Thomas, G. A., and Tsuboi, M. (1987) in *Biological Applications of Raman Spectroscopy* (Spiro, T. G. Ed.) Vol. 1, pp 81−133, Wiley-Interscience, New York.
29. Nishimura, Y., Hirakawa, A. Y., and Tsuboi, M. (1978) in *Advances in Infrared and Raman Spectroscopy* (Clark, R. J. H., and Hester, R. E., Eds.) Vol. 5, pp 217−275, Heyden, London.
30. Lord, R. C., and Thomas, G. J., Jr. (1967) *Spectrochim. Acta 23A*, 2551−2591.
31. Kubasek, W. L., Hudson, B., and Peticolas, W. L. (1985) *Proc. Natl. Acad. Sci. U.S.A.* 82, 2369−2373.
32. Fodor, S. P. A., Rava, R. P, Hays, T. R., and Spiro, T. G. (1985) *J. Am. Chem. Soc. 107*, 1520−1529.
33. Toyama, A., Takino, Y., Takeuchi, H., and Harada, I. (1993) *J. Am. Chem. Soc. 115*, 11092−11098.
34. Takeuchi, H., Watanabe, N., and Harada, I. (1988) *Spectrochim. Acta 44A*, 749−761.
35. Takeuchi, H., Watanabe, N., Satoh, Y., and Harada, I. (1989) *J. Raman Spectrosc. 20*, 233−237.
36. Asher, S. A., Ludwig, M., and Johnson, C. R. (1986) *J. Am. Chem. Soc. 108*, 3186−3197.
37. Tsuboi, M., Komatsu, M., Hoshi, J., Kawashima, E., Sekine, T., Ishido, Y., Russell, M. P., Benevides, J. M., and Thomas, G. J., Jr. (1997) *J. Am. Chem. Soc. 119*, 2025−2032.
38. Pimental, G. C., and McClellan, A. L. (1960) *The Hydrogen Bond*, W. H. Freeman and Co., San Francisco, CA.
39. Laporte, L., and Thomas, G. J., Jr. (1998) *J. Mol. Biol. 281*, 261−270.
40. Toyama, A., Hamuara, M., and Takeuchi, H. (1996) *J. Mol. Struct. 379*, 99−108.
41. Benevides, J. M., and Thomas G. J., Jr. (1983) *Nucleic Acids Res. 11*, 5747−5761.
42. Small, E. W., and Peticolas, W. L. (1971) *Biopolymers 10*, 69−88.
43. Siamwiza, M. N., Lord, R. C., Chen, M. C., Takamatsu, T., Harada, I., Matsuura, H., and Shimanouchi, T. (1975) *Biochemistry 14*, 4870−4876.
44. Overman, S. A., Aubrey, K. L., Vispo, N. S., Cesareni, G., and Thomas, G. J., Jr. (1994) *Biochemistry 33*, 1037−1042.
45. Efremov, R. G., Feofanov, A. V., and Nabiev, I. R. (1992) *J. Raman Spectrosc. 23*, 69−73.
46. Chi, Z., and Asher, S. A. (1998) *Biochemistry 37*, 2865−2872.
47. Overman, S. A., and Thomas, G. J., Jr. (1998) *Biochemistry 37*, 5654−5665.
48. Matsuno, M., Takeuchi, H., Overman, S. A., and Thomas, G. J., Jr. (1998) *Biophys. J. 74*, 3217−3225.
49. Marvin, D. A. (1998) *Curr. Opin. Struct. Biol. 8*, 150−158.
50. Casadevall, A., and Day, L. A. (1983) *Biochemistry 22*, 4831−4842.
51. Day, L. A., Casadevall, A., Prescott, B., and Thomas, G. J., Jr. (1988) *Biochemistry 27*, 706−711.
52. Overman, S. A., Aubrey, K. L., Reilly, K. E., Osman, O., Hayes, S. L., Serwer, P., and Thomas, G. J., Jr. (1998) *Biospectroscopy 4*, S47−S56.
53. Cerritelli, M. E., Cheng, N., Rosenberg, A. H., McPherson, C. E., Booy, F. P., and Steven, A. C. (1997) *Cell 91*, 271−280.
54. Aubrey, K. L., Casjens, S. R., and Thomas, G. J., Jr. (1992) *Biochemistry 31*, 11835−11842.

BI981965M